

Supporting information

An efficient detection of bilirubin in human serum through displacement approach

Nancy Singla, Manzoor Ahmad, Vishal Mahajan, Prabhpreet Singh and Subodh Kumar*

^aDepartment of Chemistry, Centre for Advanced Studies, Guru Nanak Dev University, Amritsar, Punjab, India

Figure S1: ¹ H NMR spectrum of NCI-1	Page 2
Figure S2: ¹ H NMR spectrum of Th-Y	Page 2
Figure S3: ¹ H NMR spectrum of probe THYQ	Page 3
Figure S4: ¹³ C NMR spectrum of probe THYQ	Page 3
Figure S5: HRMS of probe THYQ	Page 4
Figure S6: Emission spectra of THYQ in water- glycerol binary mixtures (λ_{ex} 420 nm); (B) Line plot of fluorescence intensity at 640 nm v/s the fraction of glycerol	Page 4
Figure S7: (A) Absorbance and (B) Emission spectra of THYQ with the change in pH; (C) The plot of the emission maxima at 500 nm v/s pH	Page 5
Figure S8: The fluorescence spectra of THYQ (10 μ M, HEPES buffer, pH 7.4) in the presence of 5 equivalents each of HSA, anions, thiols, amines and amino acids	Page 5
Figure S9: (A) The fluorescence spectra of THYQ-HSA complex; (B) Bar graph representing the FI at 555 nm in presence of 5 equivalents each of cations, anions, thiols, amines and amino acids	Page 5
Figure S10. Change in UV-Vis spectrum of THYQ (10 μ M, HEPES buffer) on addition of aliquots of HSA	Page 6
Figure S11: (A) The distribution of different species of complexes of THYQ with HSA; (B) The change in emission spectrum of HSA at 345 nm on successive addition of aliquots of probe THYQ (λ_{ex} 290 nm); (C) SPECFIT graph showing the distribution of different species of complexes of HSA with THYQ	Page 6
Figure S12: Possibility of FRET mechanism for Bilirubin (BR) detection	Page 6
Figure S13: The DLS spectra of THYQ /HSA in the presence of BR	Page 7
Figure S14: Effect of other proteins in the quantification of BR	Page 7
Table S1: Photophysical properties of THYQ (1 μ M) in solvents of varied polarity (E_T^{30} Kcal/mol)	Page 7-8
Table S2: Comparison of slopes of E_T^{30} value v/s Emission maxima of THYQ with literature reports	Page 8-9
Table S3: Comparison of performance of various fluorescence based systems for the detection of bilirubin	Page 9-10

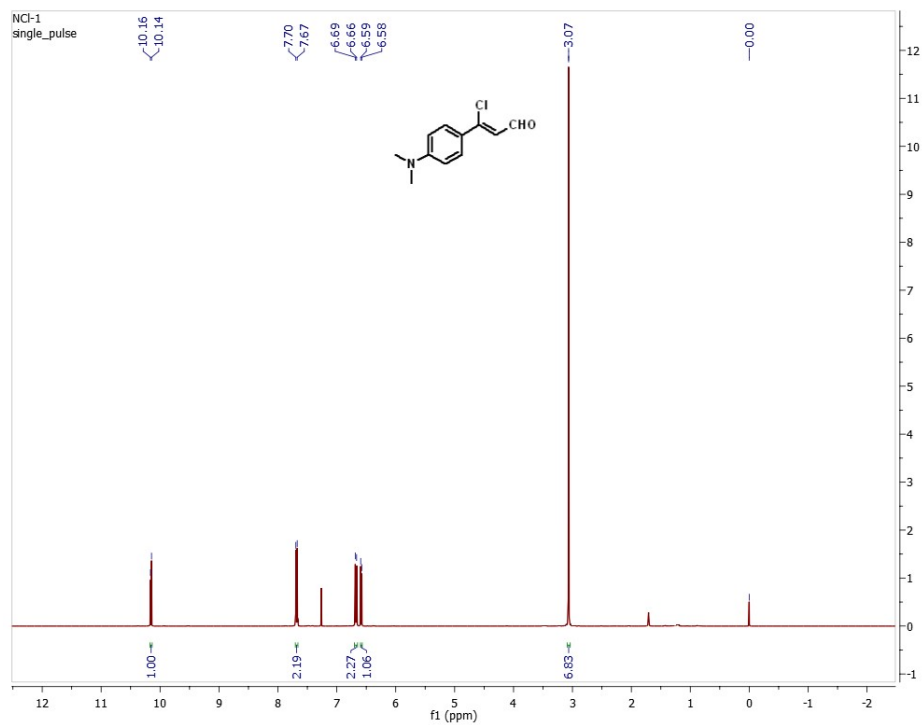


Figure S1: ^1H NMR spectrum of **NCI-1**

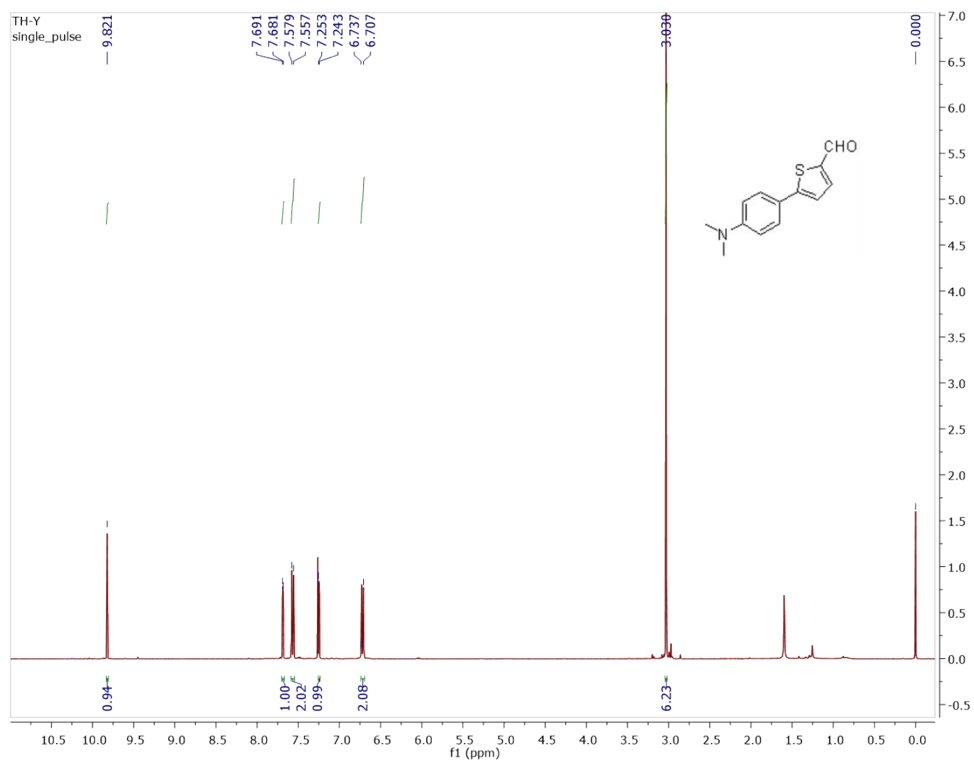


Figure S2: ^1H NMR spectrum of **TH-Y**

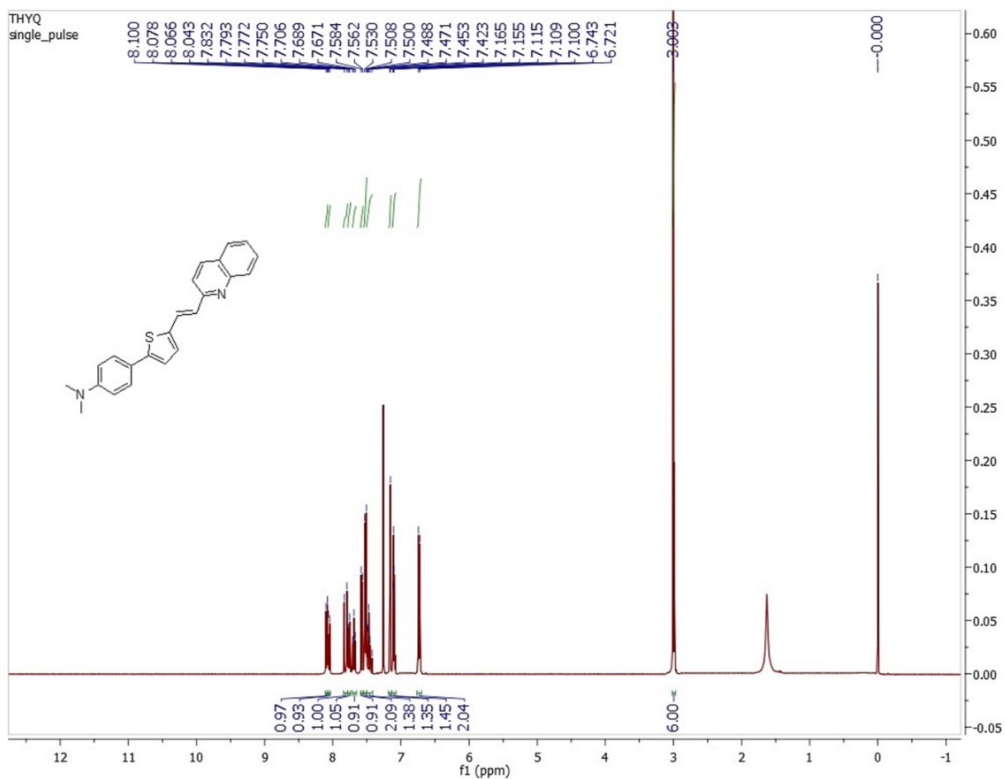


Figure S3: ^1H NMR spectrum of **THYQ**

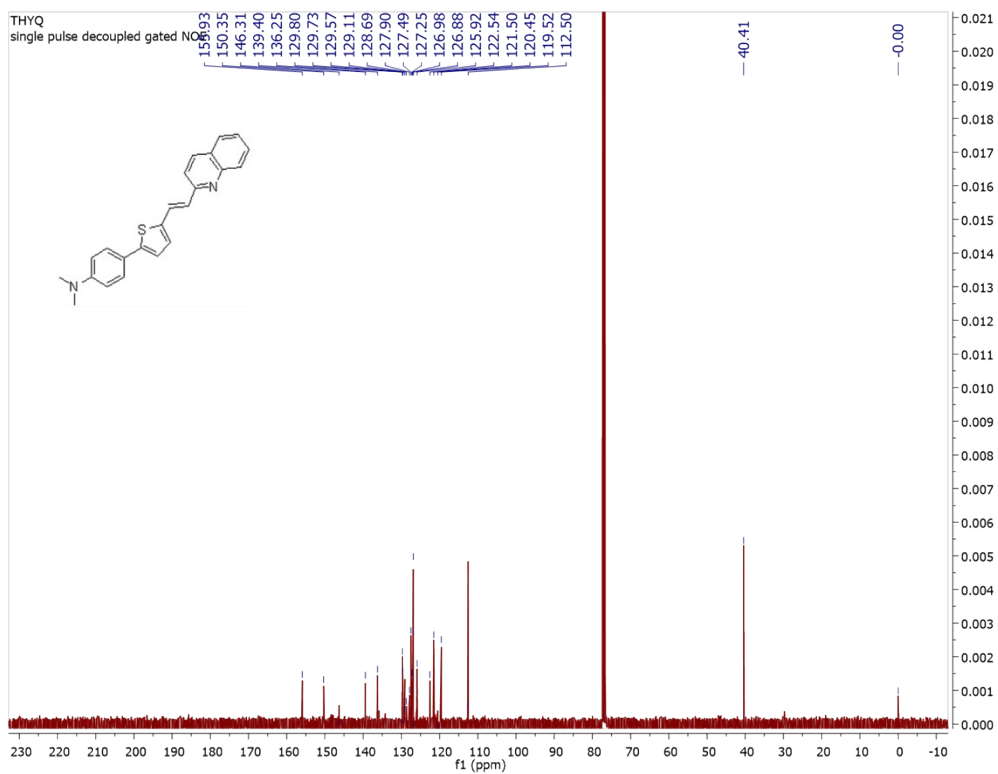


Figure S4: ^{13}C NMR spectrum of **THYQ**

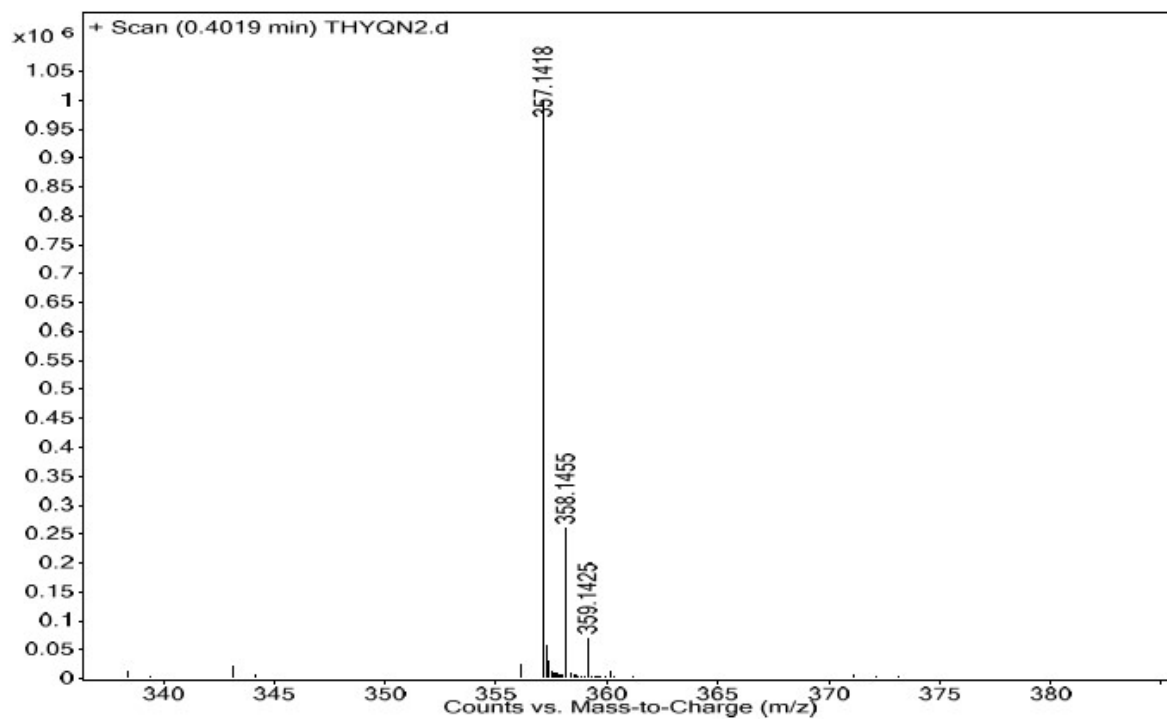


Figure S5: HRMS spectrum of **THYQ**

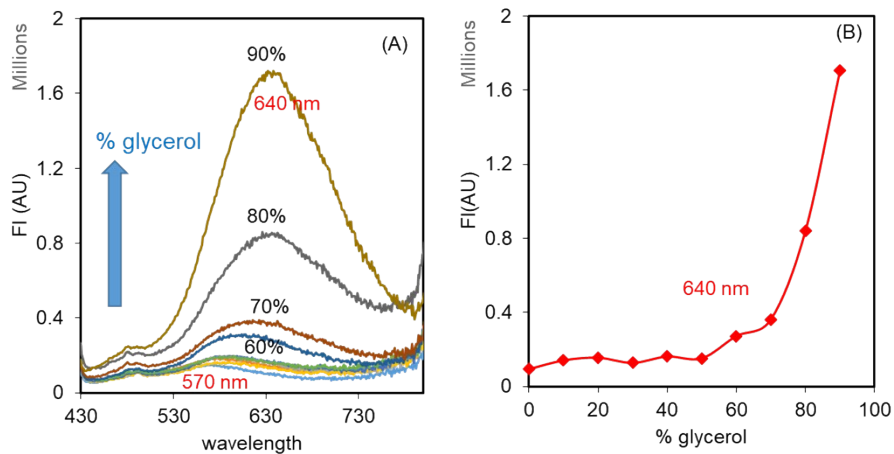


Figure S6: (A) Emission spectra of **THYQ** in water- glycerol binary mixtures (λ_{ex} 420 nm); (B) Line plot of fluorescence intensity at 640 nm v/s the fraction of glycerol

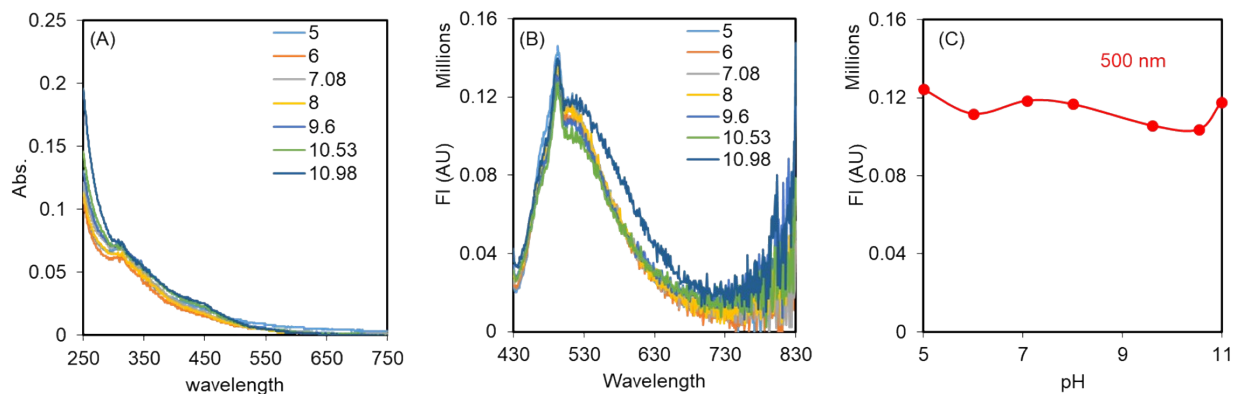


Figure S7: (A) Absorbance and (B) Emission spectra of **THYQ** with the change in pH; (C) The plot of the emission maxima at 500 nm v/s pH

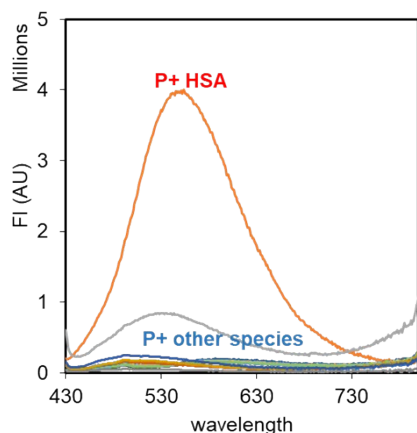


Figure S8: The fluorescence spectra of **THYQ** (10 μ M, HEPES buffer, pH 7.4) in the presence of 5 equivalents each of HSA, anions, thiols, amines and amino acids

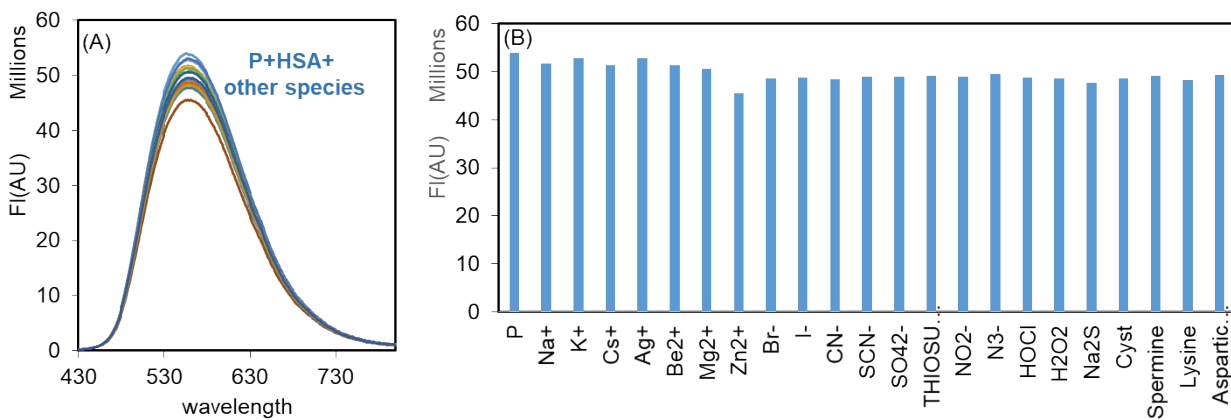


Figure S9: (A) The fluorescence spectra of **THYQ-HSA** complex; (B) Bar graph representing the FI at 555 nm in presence of 5 equivalents each of cations, anions, thiols, amines and amino acids

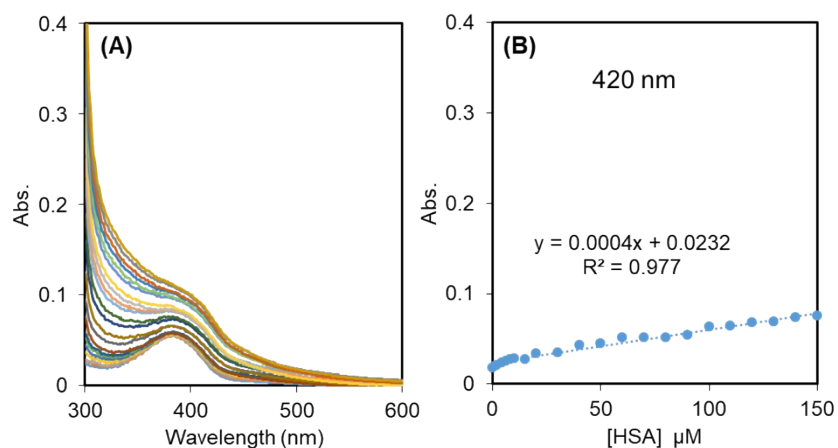


Figure S10: Change in UV-Vis spectrum of THYQ (10 μM , HEPES buffer) on addition of aliquots of HSA

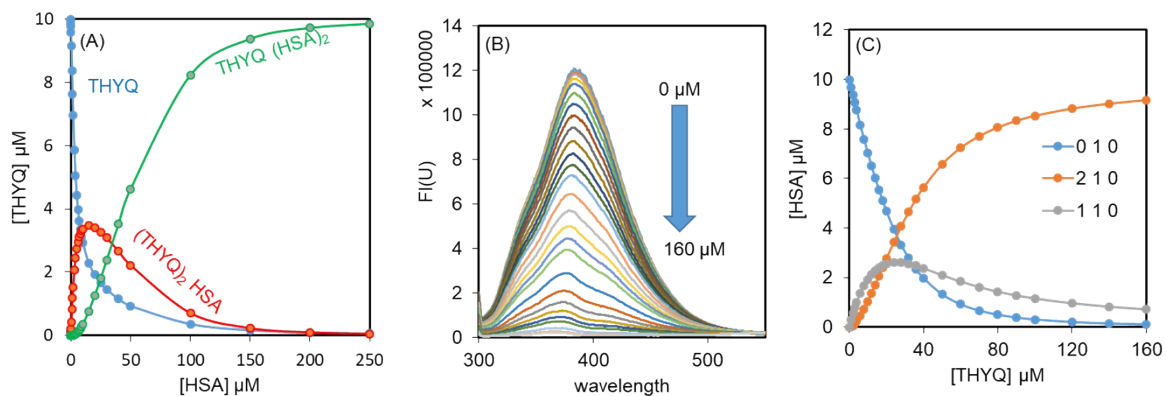


Figure S11: (A) The distribution of different species of complexes of **THYQ** with HSA; (B) The change in emission spectrum of HSA at 345 nm on successive addition of aliquots of probe **THYQ** (λ_{ex} 290 nm); (C) SPECFIT graph showing the distribution of different species of complexes of HSA with THYQ

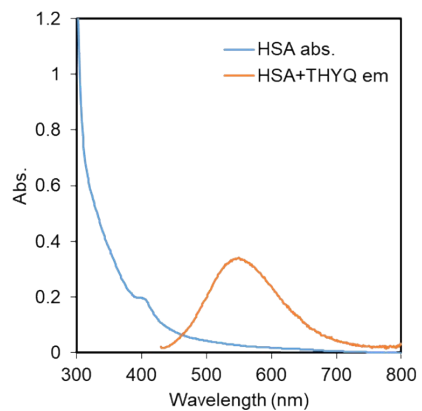


Figure S12: Possibility of FRET mechanism for Bilirubin (BR) detection

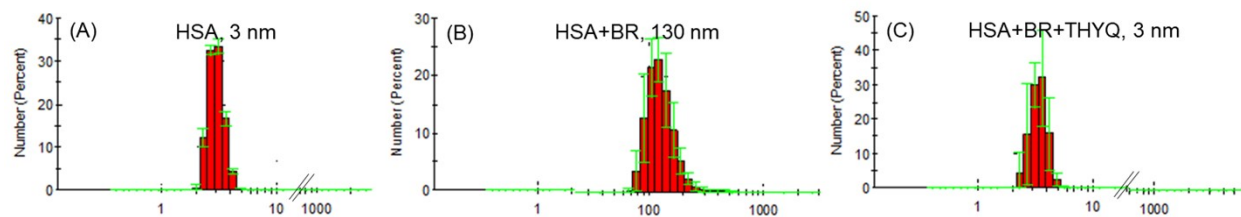


Figure S13: The DLS spectra of THYQ /HSA in the presence of BR

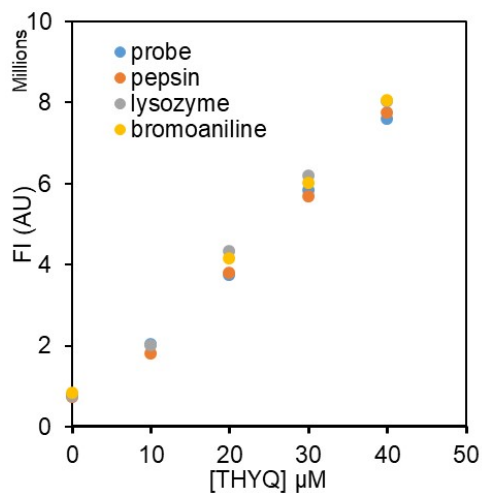


Figure S14: Effect of other proteins in the quantification of BR

Table S1. Photophysical properties of THYQ (1 μM) in solvents of varied polarities (E_T^{30} Kcal/mol)

Solvent	E_T^{30} (Kcal/mol)	$\lambda_{Abs.}$ Max (nm)	$\lambda_{Em.}$ Max (nm)	ϵ ($M^{-1} cm^{-1}$)	Φ (At 1 μM)
cyclohexane	30.9	414	510	11,900	18.38
toulene	33.9	427	527	17,100	20.34
Diethyl ether	34.5	416	538	21,900	29.61
THF	37.4	424	572	25,500	88.12
Ethyl acetate	38.1	415	570	24,700	41.76
CHCl ₃	39.1	424	555	20,200	---
DCM	40.7	422	581	28,100	52.31
acetone	42.2	427	594	27,800	84.92
DMF	43.2	435	610	29,900	70.87
DMSO	45.1	420,546	622	21,400 and 6,000	67.84
ACN	45.6	421,536	612	19,400 and 13,600	53.18

ethanol	51.9	430,537	626	19,000 and 15,300	7.70
methanol	55.4	---	636	---	7.70
Water	63.1	Broad band	weak band	6100	-

Table S2: Comparison of slopes of E_T^{30} value v/s Emission maxima of **THYQ** with literature reports

S. No.	Ref	Structure	Slope nm / E_T^{30}	S. No.	Ref	Structure	Slope nm / E_T^{30}
1	Ref 1		2.7	7	Ref 6		5.7
2	Ref 1		4.6	8	Ref 7		7.7
3	Ref 2		3.98	9	Ref 8		10.03
4	Ref 3		4.51	10	Ref 9		6.14
5	Ref 4		9.32	11	This Work		7.88
6	Ref 5		9.46				

References

1. C. Yu, X. Guo, X. Fang, N. Chen, Q. Wu, E. Hao and L. Jiao, *Dyes Pigm.*, 2022, **197**, 109838.
2. M. Collot, S. Bou, T.K. Fam, L. Richert, Y. Mély, L. Danglot and A.S. Klymchenko, *Anal. Chem.*, 2019, **91**, 1928–1935.
3. C.W. Song, U. Tamima, Y.J. Reo, M. Dai, S. Sarkar and K.H. Ahn, *Dyes Pigm.*, 2019, **171**, 107718.
4. H. Wang, L. Hu, S. Shen, K. Yu and Y. Wang, *New J. Chem.*, 2021, **45**, 21553–21556.
5. J. Yin, M. Peng, Y. Ma, R. Guo and W. Lin, *Chem. Commun.*, 2018, **54**, 12093–12096.
6. L. Yang, J. Wang, B. Liu, G. Han, H. Wang, L. Yang, J. Zhao, M.-Y. Han and Z. Zhang, *Sens. Actuators B.*, 2021, **333**, 129541.

7. Z. Zhan, W. Zhuang, Q. Lei, S. Li, W. Mao, M. Chen and W. Li, *Chem. Commun.*, 2022, **58**, 4020–4023.
8. X. Zhang, L. Yuan, J. Jiang, J. Hu, A. du Rietz, H. Cao, R. Zhang, X. Tian, F. Zhang, Y. Ma, Z. Zhang, K. Uvdal and Z. Hu, *Anal. Chem.*, 2020, **92**, 3613-3619.
9. X. Shi, S.H. P. Sung, M.M. S. Lee, R.T. K. Kwok, H.H. Y. Sung, H. Liu, J.W. Y. Lam, I. D. Williams, B. Liu and B. Zhong Tang, *J. Mater. Chem. B.*, 2020, **8**, 1516–1523.

Table S3: Comparison of performance of various fluorescence based systems for the detection of bilirubin

Sr. No	Fluorescence System	pH	FL ON/OFF	Linear range	LOD	Clinical detection Spiking /direct	[Ref], Year
Organic molecule based probes							
1.	Displacement approach	7.4	“ON”	2-80 μM	68 nM	direct	This Work
2.	Imine based	7.4	“OFF”	1 pM-500 μM	2.8 pM	spiking	1, 2017
3.	Probe+Fe ³⁺ mixture used	7.2	“ON”	0–10 μM	76 nM	direct	2, 2020
4.	Probe+Fe ³⁺ mixture used	7.4	“ON”	0–10 μM	33 nM	direct	3, 2021
5.	Amphiphilic molecule	6.5	“OFF”	0–32 μM	330 nM	spiking	4, 2023
6.	imidazole derivative	7.4	“OFF”	0–60 μM	11.74 μM	spiking	5, 2023
Nano-materials							
7.	HSA stabilized gold nanoclusters	7.4	“OFF”	1–50 μM	248 nM	spiking	6, 2014
8.	Peroxidase method	8.0	“OFF”	0.03-5.0 μM	10 nM	spiking	7, 2018
9.	S,N-doped carbon dots + Fe ³⁺	2.5	“ON”	0.2 -2.0 nM	0.12 nM	spiking	8, 2018
10.	BSA stabilized copper nanocluster + Fe ³⁺	11.4	“ON”	0-70 μM	6.62 nM	spiking	9, 2018
11.	L-cysteine capped Mn doped ZnS ₂ quantum dots	4.7	“OFF”	10.99 - 63.84 μM	1800 nM	spiking	10, 2019
12.	N doped carbon dots	7.4	“OFF”	0-45 μM	89 nM	spiking	11, 2021
13.	glutathione capped copper nanoclusters	ND	“OFF”	9-800 μM	148 nM	*ND	[12], 2021
14.	TPE hydrogel	7.4	“OFF”	0-8 μM	25 nM	*ND	[13], 2022
15.	competitive binding of Cu ²⁺	5.0	“ON”	0.7–3.6 μM	85 nM	spiking	[14], 2022

*ND = not determined

References

1. S. Ellairaja, K. Shenbagavalli, S. Ponmariappan and V.S. Vasantha, *Biosens. Bioelectron.*, 2017, **91**, 82–88.

2. E. Ahmmed, A. Mondal, A. Sarkar, S. Chakraborty, S. Lohar, N.C. Saha, K. Dhara and P. Chattopadhyay, *ACS Appl. Bio Mater.*, 2020, **3**, 4074-4080.
3. E. Ahmmed, A. Mondal, N.C. Saha, K. Dhara and P. Chattopadhyay, *Anal. Methods*, 2021, **13**, 5651–5659.
4. S. Qi, X. He, S. Zhang, P. Xu, M. Su, B. Dong and B. Song, *Anal. Chim. Acta*, 2023, **1238**, 340657.
5. K. Anusuyadevi and S. Velmathi, *Anal. Chim. Acta*, 2023, **1239**, 340678.
6. M. Santhosh, S. R. Chinnadayala, A. Kakoti and P. Goswami, *Biosens. Bioelectron.*, 2014, **59**, 370–376.
7. M. Zhang, L. Xu, Q. Ma, H. Yu, H. Fang, Z. Lin, Q. Zhang and Z. Chen, *ACS Appl. Mater. Interfaces*, 2018, **10**, 42155–42164.
8. R.R. Anjana, J.S. Anjali Devi, M. Jayasree, R.S. Aparna, B. Aswathy, G.L. Praveen, G.M. Lekha and G. Sony, *Microchim. Acta*, 2018, **185**, 1-11.
9. M. Jayasree, R.S. Aparna, R.R. Anjana, J.S. Anjali Devi, Nebu John, K. Abha, A. Manikandan and S. George, *Anal. Chim. Acta*, 2018, **1031**, 152-160.
10. K. Abha, J. Nebu, J.S. Anjali Devi, R.S. Aparna, R.R. Anjana, A.O. Aswathy and S. George, *Sens. Actuators B.*, 2019, **282**, 300–308.
11. N. Nandi, S. Gaurav, P. Sarkar, S. Kumar and K. Sahu, *ACS Appl. Bio Mater.*, 2021, **4**, 5201–5211.
12. S. K. Anand, M. R. Mathew and K. G. Kumar, *J Photochem Photobiol, A.*, 2021, **418**, 113379.
13. B. Wang, X. Q. Zhou, L. Li, Y. X. Li, L. P. Yu and Y. Chen, *Sens. Actuators B.*, 2022, **369**, 132392.
14. B. Barik and S. Mohapatra, *Anal. Biochem.*, 2022, **654**, 114813.